



Optical Excitation of Nuclear Spin Coherence in Tm³⁺:YAG

Anne Louchet, Yann Le Du, Fabien Bretenaker, Thierry Chanelière, Fabienne Goldfarb, Ivan Lorgeré, Jean-Louis Le Gouët, Olivier Guillot-Noël, Philippe Goldner

► To cite this version:

Anne Louchet, Yann Le Du, Fabien Bretenaker, Thierry Chanelière, Fabienne Goldfarb, et al.. Optical Excitation of Nuclear Spin Coherence in Tm³⁺:YAG. *Physical Review B: Condensed Matter and Materials Physics*, American Physical Society, 2008, 77 (19), 10.1103/PhysRevB.77.195110. hal-00179895v2

HAL Id: hal-00179895

<https://hal.archives-ouvertes.fr/hal-00179895v2>

Submitted on 23 Apr 2019

HAL is a multi-disciplinary open access archive for the deposit and dissemination of scientific research documents, whether they are published or not. The documents may come from teaching and research institutions in France or abroad, or from public or private research centers.

L'archive ouverte pluridisciplinaire **HAL**, est destinée au dépôt et à la diffusion de documents scientifiques de niveau recherche, publiés ou non, émanant des établissements d'enseignement et de recherche français ou étrangers, des laboratoires publics ou privés.

Optical excitation of nuclear spin coherence in a Tm^{3+} :YAG crystal

A. Louchet, Y. Le Du, F. Bretenaker, T. Chanelière, F. Goldfarb, I. Lorgeré, and J.-L. Le Gouët
Laboratoire Aimé Cotton, CNRS-UPR 3321, Univ. Paris-Sud, Bâtiment 505, 91405 Orsay Cedex, France

O. Guillot-Noël and Ph. Goldner

*Laboratoire de Chimie de la Matière Condensée de Paris, CNRS-UMR 7574, Ecole Nationale Supérieure de Chimie de Paris (ENSCP),
 11 rue Pierre et Marie Curie, 75231 Paris Cedex 05, France*

(Received 7 February 2008; published 14 May 2008)

A thulium-doped crystal is experimentally shown to be an excellent candidate for broadband quantum storage in a solid-state medium. The nuclear spin coherence is optically excited, detected, and characterized in such a crystal. The lifetime of the spin coherence—the potential storage entity—is measured by means of a new Raman echo protocol to be about 300 μs over a wide range of ground state splittings. This flexibility, which is attractive for broadband operation and well fitted to existing quantum sources, results from the simple hyperfine structure, which contrasts to Pr- and Eu-doped crystals.

DOI: [10.1103/PhysRevB.77.195110](https://doi.org/10.1103/PhysRevB.77.195110)

PACS number(s): 78.40.Pg, 42.50.Gy, 42.50.Md, 78.30.Ly

So far, the mapping of a quantum state of light onto an atomic ensemble has been implemented in atomic vapors¹ and cold atom clouds.² The extension to solid state media has been actively pursued. In this context, rare-earth ion-doped crystals (REICs) have been proposed as candidates for optical quantum storage.^{3–6} To some extent, REICs at low impurity concentrations are similar to atomic vapors with the advantage of no atomic diffusion. In the frame of classical optics, those materials have been extensively investigated for optical data storage⁷ and data processing^{8,9} because of their long optical coherence lifetimes at low temperatures.

Most quantum memory for light (QML) protocols rely on the transfer of a quantum state of light into a long-lived spin coherence that is free from decoherence via spontaneous emission. This can be achieved in a Λ -type three-level system wherein two hyperfine or spin sublevels are optically connected to a common upper level. The presence of a Λ system ensures efficient coupling between light and matter together with long storage times. A Λ system also represents a basic device where, in a simple way, the transition to be excited by the quantum field can be triggered for storage or restitution by an external control field.

It is noteworthy that the essence of Λ -system operation, namely, the optical excitation of nuclear spin, has been practised in REICs for almost 30 years, but always in praseodymium- or europium-doped crystals. In addition to hyperfine splitting and population relaxation measurements,^{10–13} these works also involve the optical driving and control of the nuclear spin coherence, which is more closely related to optical quantum storage. Those coherence-oriented investigations include coherent Raman beats,^{14,15} Raman echoes,^{16,17} stimulated Raman adiabatic passage (STIRAP)¹⁸ and electromagnetically induced transparency (EIT).¹⁹ Derived from EIT, the “stopped light” protocol represents the ultimate step toward QML and was also demonstrated in Pr-doped crystals.^{3,4} However, quantum storage demonstration in Pr- or Eu-doped compounds is limited by the smallness of their hyperfine structure, which does not really match the bandwidth of existing quantum sources. We recently demonstrated the existence of a Λ system with adjustable ground state splitting in thulium-doped yttrium alu-

minum garnet (YAG).²⁰ Widely adjustable splitting might help to match the bandwidth of existing quantum sources. In this paper, we optically excite, characterize and detect the nuclear spin coherence in the electronic ground state of a Tm-doped crystal.

In crystals doped with Pr^{3+} or Eu^{3+} , Λ systems are built on the hyperfine structure of the ground level with a sublevel splitting up to a few tens of megahertz. This spacing represents the memory bandwidth. Indeed, the two transitions of Λ cannot be polarization selected and, thus, only differ by their frequency. Therefore, in order to excite only the relevant single transition, the incoming signal must be spectrally narrower than the splitting. Applying an external magnetic field would increase the splitting and the memory bandwidth but would split each hyperfine level into two nuclear spin sublevels, thus drastically complexifying the level system. Besides, only dye lasers are available at Pr^{3+} and Eu^{3+} operating wavelengths, i.e., 606 and 580 nm, respectively, in yttrium orthosilicate (YSO). Because of the high frequency noise generated by a dye jet, it is a challenging task to achieve the subkilohertz linewidth sources that are needed to benefit from the long optical coherence lifetime. This limits the realization to laboratory proof of principle. Although some groups successfully built such laser sources,^{21,22} it is worth devising an alternative approach.

The thulium rare earth ion actually gathers together many advantages that make it especially attractive. First, its 793 nm wavelength falls within reach of easily stabilized semiconductor lasers, unlike those of Pr and Eu. Then, its $I = 1/2$ nuclear spin gives rise, under an external magnetic field, to a simple straightforward four-level optical system in which a Λ system can be selected. Moreover, because of this simple structure, the sublevel splitting can be easily controlled by the external magnetic field. This crystal could therefore be used as an atomic quantum memory that is adapted to the bandwidth of existing quantum sources. For these reasons, thulium-doped materials are favorable alternatives to Pr- and Eu-doped compounds for quantum storage applications, with the triple advantage of a tractable wavelength, a simple level system, and an adjustable ground state splitting.

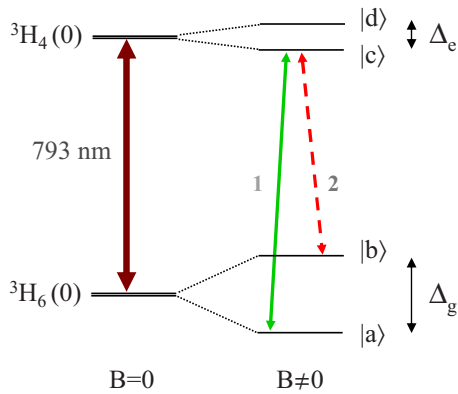


FIG. 1. (Color online) Λ system in Tm:YAG built on the nuclear Zeeman structure by application of an external magnetic field.

The application of a magnetic field lifts the nuclear spin degeneracy, but this is not enough to obtain a Λ system (cf. Fig. 1). Indeed, optical excitation cannot flip a nuclear spin, as expressed by a selection rule on the nuclear spin projection m_I . However, the coupling of the electronic Zeeman effect and hyperfine interaction enhances the nuclear Zeeman effect and gives rise to nuclear gyromagnetic tensor anisotropy. If the anisotropy is different between the ground and the upper electronic levels, the nuclear spin eigenvectors also differ between those two levels. As a consequence, the nuclear spin selection rule is relaxed. In a YAG crystal, Tm ions are doped into low symmetry sites (D_2) with a gyromagnetic tensor anisotropy that is much larger in the electronic ground state than in the excited state.²⁰ For an appropriate orientation of the applied magnetic field, the optical transition probability ratio along the two legs of the Λ can be optimized. In 2005, Guillot-Noël *et al.*²³ theoretically showed that for an adequate external field orientation, the branching ratio of the two transition probabilities reaches 0.24 in two crystalline sites out of the three that can be selected by laser beam polarization. In 2006, we directly measured this optimal branching ratio to be 0.13 ± 0.02 , proving that the nuclear spin selection rule is effectively relaxed.^{20,24} An adjustable Λ system can now be built, involving both ground state sublevels coupled to one of the two excited state sublevels.

The magnetic field B being oriented to optimize the branching ratio, the nuclear Zeeman sensitivity can be measured with the help of hole burning spectroscopy. We find $\Delta_g/B=36$ MHz/T and $\Delta_e/B=16$ MHz/T, where Δ_g and Δ_e stand for the ground and the excited electronic state splittings, respectively. We also observe that, as depicted in Fig. 2, the side hole and antihole widths exceed the hole width at the burning frequency and linearly vary with the magnetic field amplitude with a slope of 0.99 MHz/T in the ground state and 0.093 MHz/T in the excited state. We ascribe this broadening to spatial variations in the magnetic field and substitution site relative orientation. The external field orientation that optimizes the transition probability branching ratio is close to the direction of minimum splitting, and, accordingly, nearly orthogonal to the main component of the gyromagnetic tensor. This is the reason why we measure a Zeeman sensitivity of 36 MHz/T, although the main gyro-

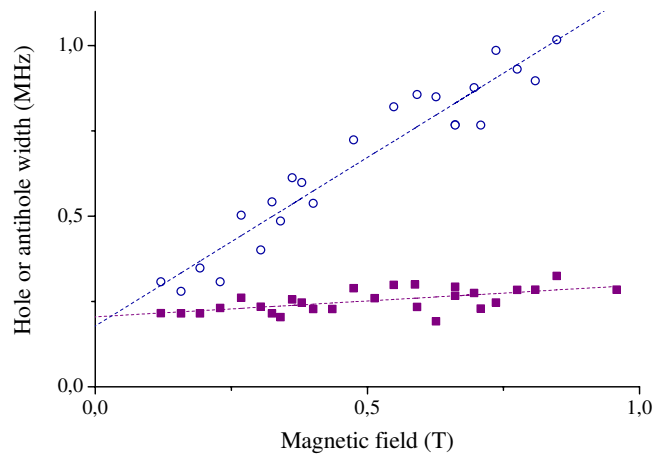


FIG. 2. (Color online) Inhomogeneous broadening of side hole at detuning Δ_e (filled squares) and of antiholes at detuning Δ_g (empty circles). The 200 kHz hole and antihole residual width at zero field is assigned to chirped readout at 35 GHz/s. The dashed lines are fitted to the data. Their slope is 0.99 MHz/T for the antihole and 0.093 MHz/T for the hole.

magnetic coefficient reaches 400 MHz/T in the ground state. As a consequence, a slight tilt of the field with respect to the site frame entails a dramatic splitting variation. At 1 T, a 1 mrad misorientation is enough to generate a 0.3 MHz splitting deviation in the ground state. At the moment, it is not clear whether the observed inhomogeneous broadening is caused by site orientation disorder or by applied field orientational nonuniformity. The ground state width appears to be ten times more sensitive to the magnetic field magnitude than the excited state width. Indeed, the gyromagnetic tensor is much less anisotropic in the upper level than in the ground state. The ratio is consistent with an isotropic misorientation model.

We now turn to investigate the spin coherence with optical means. Initially, the two ground state sublevels are equally populated and the optical transition frequency is distributed over a 25-GHz-wide inhomogeneously broadened absorption profile. Within this huge bandwidth, we select a narrow interval, which is smaller than $\Delta_g - \Delta_e$, over which we prepare the ions by pumping them into a single sublevel. This way, the two-photon excitation is optimized. Optical pumping is accomplished by a sequence of 100 μ s chirped pulses. Then, we excite the ground state spin coherence with a 10 μ s bichromatic laser pulse. The two frequency components ω_1 and ω_2 , which are tuned to the Λ -system optical transitions, are separated by Δ_g to satisfy the two-photon resonance condition. If all atoms remain phased together, one could monitor the spin coherence evolution by coherent forward Raman scattering: A long rectangular monochromatic pulse at frequency ω_1 excites one transition of the Λ and converts part of the spin coherence into an optical coherence along the other transition. The resulting optical emission could be detected as a beatnote at frequency Δ_g against the probe pulse. Unfortunately, the spin coherences evolve at different rates, according to the inhomogeneous broadening we observed in Fig. 2. This makes the beatnote vanish on the time scale of the excitation pulse duration. In order to re-

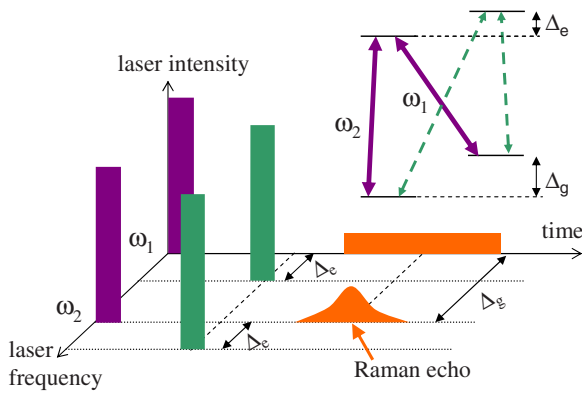


FIG. 3. (Color online) Raman echo pulse sequence for photon echo elimination using the two Λ systems. The second pulse is detuned from the first one by the excited state splitting Δ_e but still satisfies the two-photon resonance. Inset: Four-level system. The first and second pulse frequencies (ω_1, ω_2) and ($\omega_1 + \Delta_e, \omega_2 + \Delta_e$) are respectively depicted as solid and dashed arrows.

cover the optical signature of the spin coherences, we resort to the Raman echo procedure.^{16,17,25–27} We apply an additional bichromatic pulse, which is resonant with the two-photon transition, at the midtime between initial excitation and final probing. This pulse reverses the spin coherence time evolution, so that, at the moment of probing, the spin coherences are phased together again and give rise to an optical emission. The Raman echo signal is observed by means of real-time fast Fourier transform.

The Raman echo is contaminated by two-pulse photon echo signals. The photon echo signal at frequency ω_2 beats with the detection pulse, overlapping temporally and spectrally with the Raman echo. In previous Raman echo experiments,¹⁶ the photon echo was rejected by the angular separation of the various signals. In the present work, we have preferred a strictly collinear geometry that optimizes the spatial mode matching of the various beams. Then, to get rid of the photon echo, we propose a new protocol. While maintaining an efficient driving of spin coherences, we detune the two frequencies of the rephasing pulse so that they are optically resonant with the other Λ system of our four-level system (cf. Fig. 3).

The system is illuminated with an extended cavity diode laser (ECDL) that operates at 793 nm and is stabilized on a high-finesse Fabry–Perot cavity through a Pound–Drever–Hall servoloop down to 200 Hz over 10 ms.²⁸ The laser is amplified with a semiconductor tapered amplifier (Toptica BoosTA). A polarizing cube splits the beam. Each component is double-passed through an acousto-optic modulator (AOM) that is centered at 110 MHz (AA OptoElectronics). The two AOMs are driven by a dual-channel 1 gigasample/s waveform generator (Tektronix AWG520) that can provide arbitrary amplitude and phase shaping. In this experiment, each channel feeds one frequency shift at a time. After passing twice through the AOMs, the split beams come back to the cube, where they merge into a fixed-direction single beam carrying bichromatic excitation. A common polarization direction is given by a Glan prism. The recombined beam is finally coupled into a 2-m-long single-mode fiber.

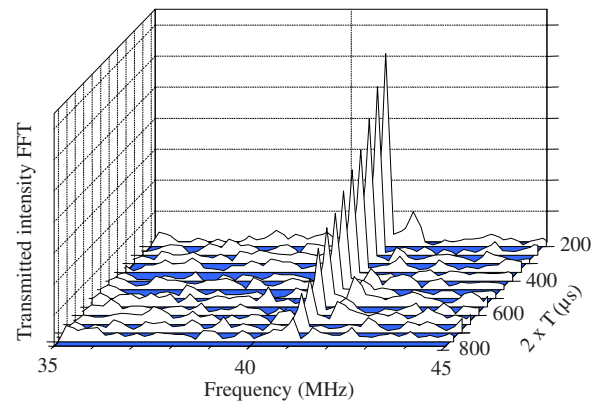


FIG. 4. (Color online) Raman echo signals for $\Delta_g = 41$ MHz as delay time T is increased from 100 to 400 μ s. The spin coherence lifetime is derived from the exponential decay of this signal.

The light polarization direction is adjusted with a half-wave plate to maximize the Rabi frequency. It is then focused on a 5-mm-thick, 0.1 at. % Tm^{3+} :YAG sample cooled down to 1.7 K in an Oxford Spectromag cryostat. The magnetic field that is generated by superconducting coils is applied in the direction optimizing the branching ratio.²⁴ The spot diameter on the crystal is 80 μ m. The transmitted light is collected on an avalanche photodiode (Hamamatsu C5460 or C4777) that is protected from strong excitation damaging light pulses by a third acousto-optic modulator used as a shutter.

Raman echo experiments yield the spin coherence lifetime T_2 . The delay of the two bichromatic pulses is denoted as T . The Raman signal decays with T as e^{-2T/T_2} . As an example, Fig. 4 shows the Raman signal decay for a $\Delta_g = 41$ MHz ground state splitting. We measure the spin coherence lifetime for different ground state splittings in Tm^{3+} :YAG. The low efficiency of the Raman echo process accounts for the low signal to noise ratio. Thanks to the double-pass setup, the two AOMs' 50 MHz nominal bandwidth is extended to 100 MHz. However, 100 MHz is the upper boundary not for Δ_g but for $\Delta_g + \Delta_e \approx 1.4\Delta_g$, since the excitation sequence is comprised of four different frequencies: ω_1 and $\omega_2 = \omega_1 - \Delta_g$ for the first pulse and $\omega_1 + \Delta_e$ and $\omega_1 - \Delta_g + \Delta_e$ for the second pulse (cf. Fig. 3). We have been able to reach a ground state splitting Δ_g of up to 83 MHz. We show in Fig. 5 that the spin coherence lifetime does not significantly depend on the ground state splitting, remaining close to 300 μ s over a 80 MHz range. The error bars correspond to the standard error that is deduced from a least-squares fit. We also measured the spin coherence lifetime in the excited state to be 540 ± 35 μ s for a 16.4 MHz excited state splitting with a similar Raman echo sequence. This lifetime is close to the population lifetime of the upper electronic state.²⁹ With a population lifetime of 800 μ s, the intrinsic spin coherence lifetime turns out to exceed 1 ms. The mechanisms responsible for spin decoherence in ground and excited states need to be unveiled by further studies.

Controlled reversible inhomogeneous broadening (CRIB)³⁰ or EIT experiments would be another step toward the demonstration of thulium-doped crystals as quantum memories. In materials such as ion-doped crystals, EIT might be regarded as a challenging operation. Indeed, overcoming

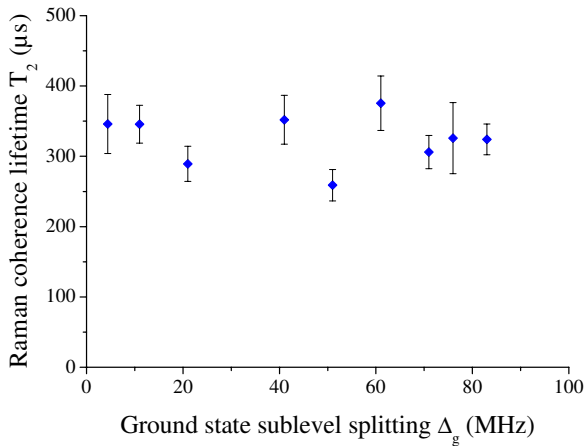


FIG. 5. (Color online) Measurement of the spin coherence lifetime for different ground state splittings, from 4 to 83 MHz. The error bars correspond to the standard error that is deduced from a least-squares fit.

the optical inhomogeneous linewidth by the coupling field Rabi frequency is known to be needed for an efficient EIT.³¹ However, atoms that are far from optical resonance with the probe do not affect EIT, provided that their ground state sublevels are equally populated. Therefore, the effective inhomogeneous width to be considered essentially corresponds to the population-unbalanced atoms that are close to optical resonance. Those atoms cover a spectral interval that is much narrower than the inhomogeneously broadened absorption line. In either Pr^{3+} -, Eu^{3+} -, or Tm^{3+} -doped crystals, this feature is essential to discard nonresonant ions. In Eu^{3+} - and

Pr^{3+} -doped crystals, resonant atoms tend to be pumped to the third sublevel by the driving fields and have to be repumped back to the selected Λ system^{3,4} with the help of an auxiliary beam. This preparation procedure only affects atoms that are close to optical resonance. In Tm^{3+} -doped crystals, this preparation step can probably be avoided since the ground state is split into two sublevels only.

The linear Stark shift should be very small in Tm^{3+} :YAG owing to the D_2 site symmetry. Therefore, inhomogeneous broadening is difficult to reverse, which is not appropriate for CRIB. Alternatively, one can consider to dope Tm ions into host matrices that exhibit a lower site symmetry such as Y_2O_3 or LiNbO_3 . In these matrices, the Stark effect exists, allowing the building of an artificial inhomogeneous broadening by the application of an electric field gradient. In LiNbO_3 , the oscillator strength is found to be 50 times stronger than in YAG.³²

To conclude, we have optically excited, detected and characterized a nuclear spin coherence in a thulium-doped crystal. In addition to presenting a convenient absorption wavelength and a simple and adjustable Λ -type three-level system, Tm^{3+} :YAG also offers long ground state spin coherence lifetimes, at splittings of up to 80 MHz and probably much higher. This lifetime stability over a wide frequency range proves the crystal adequacy to existing quantum sources.^{33,34} The precise origin of the spin inhomogeneous broadening is still to be clarified. Given its specific properties, thulium can be considered as an excellent candidate for quantum storage in a solid, challenging the previously studied praseodymium or europium.

¹B. Julsgaard, A. Kozhekin, and E. S. Polzik, *Nature (London)* **413**, 400 (2001).

²A. Kuzmich, W. P. Bowen, A. D. Boozer, A. Boca, C. W. Chou, L.-M. Duan, and H. J. Kimble, *Nature (London)* **423**, 731 (2003).

³A. V. Turukhin, V. S. Sudarshanam, M. S. Shahriar, J. A. Musser, B. S. Ham, and P. R. Hemmer, *Phys. Rev. Lett.* **88**, 023602 (2001).

⁴J. J. Longdell, E. Fraval, M. J. Sellars, and N. B. Manson, *Phys. Rev. Lett.* **95**, 063601 (2005).

⁵A. L. Alexander, J. J. Longdell, M. J. Sellars, and N. B. Manson, *Phys. Rev. Lett.* **96**, 043602 (2006).

⁶S. Hastings-Simon, M. Staudt, M. Afzelius, P. Baldi, D. Jaccard, W. Tittel, and N. Gisin, *Opt. Commun.* **266**, 716 (2006).

⁷M. Mitsunaga, R. Yano, and N. Uesugi, *Opt. Lett.* **16**, 1890 (1991).

⁸K. D. Merkel and W. R. Babbitt, *Opt. Lett.* **23**, 528 (1998).

⁹G. Gorju, V. Crozatier, I. Lorgeré, J.-L. Le Gouët, and F. Bretenaker, *IEEE Photon. Technol. Lett.* **17**, 2385 (2005).

¹⁰L. E. Erickson, *Phys. Rev. B* **16**, 4731 (1977).

¹¹W. R. Babbitt, A. Lezama, and T. W. Mossberg, *Phys. Rev. B* **39**, 1987 (1989).

¹²R. Klieber, A. Michalowski, R. Neuhaus, and D. Suter, *Phys. Rev. B* **68**, 054426 (2003).

¹³O. Guillot-Noël, Ph. Goldner, Y. Le Du, P. Loiseau, B. Julsgaard, L. Rippe, and S. Kröll, *Phys. Rev. B* **75**, 205110 (2007).

¹⁴R. M. Shelby, A. C. Tropper, R. T. Harley, and R. M. Macfarlane, *Opt. Lett.* **8**, 304 (1983).

¹⁵T. Blasberg and D. Suter, *Opt. Commun.* **109**, 133 (1994).

¹⁶B. S. Ham, M. S. Shahriar, M. K. Kim, and P. R. Hemmer, *Opt. Lett.* **22**, 1849 (1997).

¹⁷A. L. Alexander, J. J. Longdell, and M. J. Sellars, *J. Opt. Soc. Am. B* **24**, 2479 (2007).

¹⁸J. Klein, F. Beil, and T. Halfmann, *Phys. Rev. Lett.* **99**, 113003 (2007).

¹⁹B. S. Ham, P. R. Hemmer, and M. S. Shahriar, *Opt. Commun.* **144**, 227 (1997).

²⁰F. de Seze, A. Louchet, V. Crozatier, I. Lorgeré, F. Bretenaker, J.-L. Le Gouët, O. Guillot-Noël, and Ph. Goldner, *Phys. Rev. B* **73**, 085112 (2006).

²¹M. J. Sellars, R. S. Meltzer, P. T. H. Fisk, and N. B. Manson, *J. Opt. Soc. Am. B* **11**, 1468 (1994).

²²R. Klieber, A. Michalowski, R. Neuhaus, and D. Suter, *Phys. Rev. B* **67**, 184103 (2003).

²³O. Guillot-Noël, Ph. Goldner, E. Antic-Fidancev, and J.-L. Le Gouët, *Phys. Rev. B* **71**, 174409 (2005).

²⁴A. Louchet, J. S. Habib, V. Crozatier, I. Lorgeré, F. Goldfarb, F. Bretenaker, J.-L. Le Gouët, O. Guillot-Noël, and P. Goldner,

- Phys. Rev. B **75**, 035131 (2007).
- ²⁵S. R. Hartmann, IEEE J. Quantum Electron. **4**, 802 (1968).
- ²⁶P. Hu, S. Geschwind, and T. M. Jedju, Phys. Rev. Lett. **37**, 1357 (1976).
- ²⁷K. P. Leung, T. W. Mossberg, and S. R. Hartmann, Phys. Rev. A **25**, 3097 (1982).
- ²⁸V. Crozatier, F. de Seze, L. Haals, F. Bretenaker, I. Lorgeré, and J.-L. Le Gouët, Opt. Commun. **241**, 203 (2004).
- ²⁹R. M. Macfarlane, Opt. Lett. **18**, 1958 (1993).
- ³⁰S. A. Moiseev and S. Kröll, Phys. Rev. Lett. **87**, 173601 (2001).
- ³¹E. Kuznetsova, O. Kocharovskaya, P. Hemmer, and M. O. Scully, Phys. Rev. A **66**, 063802 (2002).
- ³²R. Krishna Mohan, T. Chang, M. Tian, S. Bekker, A. Olson, C. Ostrander, A. Khallaayoun, C. Dollinger, W. R. Babbitt, Z. Cole, R. R. Reibel, K. D. Merkel, Y. Sun, R. Cone, F. Schlottau, and K. H. Wagner, J. Lumin. **127**, 116 (2007).
- ³³J. Shapiro, New J. Phys. **4**, 47 (2002).
- ³⁴F. König, E. J. Mason, F. N. C. Wong, and M. A. Albota, Phys. Rev. A **71**, 033805 (2005).